Synthetic and Structural Studies of Nonametallic *tert*-Butoxide Mixed-Metal Complexes of Yttrium, Europium, and Sodium: X-ray Crystal Structures of a New Class of $LnNa_8(OR)_{10}X$ Complexes (Ln = Y, Eu; R = CMe_3; X = Cl, OH)

William J. Evans,*[1a] Mark S. Sollberger,*[1b] and Joseph W. Ziller[1a]

Contribution from the Department of Chemistry, University of California, Irvine, Irvine, California 92717, and Fred L. Hartley Research Center, Unocal Corporation, P.O. Box 76, Brea, California 92621

Received September 4, 1992

Abstract: $LnCl_3$ (Ln = Y, Eu) reacts with 10 equiv of $NaOCMe_3$ in THF to form $LnNa_8(OCMe_3)_{10}Cl$, which can be isolated in 70–90% yield by removal of solvent, washing with hexane, and extraction with toluene. $EuNa_8(OCMe_3)_{10}Cl$ (**1**) crystallizes from toluene in space group *Pbca* with unit cell parameters at 203 K of a = 20.395(4) Å, b = 27.506(5) Å, c = 21.496(4) Å, V = 12059(4) Å^3, and D_{calcd} = 1.21 g cm^{-3} for Z = 8. Least-squares refinement of the model based on 4844 reflections ($|F_o| > 4.0\sigma(|F_o|)$) converged to a final R_F = 6.4%. $YNa_8(OCMe_3)_{10}Cl$ (**2**) crystallizes from toluene in space group *Pbca* with unit cell parameters at 203 K of a = 20.270(3) Å, b = 27.332(4) Å, c = 21.409(3) Å, V = 11861(3) Å^3, and Z = 8 for D_{calcd} = 1.16 g cm^{-3}. Least-squares refinement of the model based on 4877 observed reflections converged to a final R_F = 8.9%. The nine metals in **1** and **2** describe a capped square antiprism which has the lanthanide metal in the capping position. The metal atoms are linked by eight μ_3-$OCMe_3$ groups and one μ_4-$OCMe_3$ group which caps the square face opposite the lanthanide capping position. One terminal $OCMe_3$ group is attached to the lanthanide metal center. The chloride atom in **1** occupies a position inside the polyhedron of metals and is located 0.93 Å below the Na_4 plane closest to europium and 2.02 Å above the other Na_4 plane. In **2**, the chloride is similarly situated with analogous (Na_4 plane)–Cl distances of 0.82 and 2.12 Å, respectively. An isostructural hydroxide analog of **1** and **2**, $YNa_8(OCMe_3)_{10}(OH)$ (**3**), has also been isolated. Complex **3** crystallizes from toluene in space group *Pbca* with unit cell parameters at 295 K of a = 20.423(3) Å, b = 27.370(5) Å, c = 21.633(4) Å, V = 12 092(4) Å^3, and Z = 8 for D_{calcd} = 1.12 g cm^{-3}. Least-squares refinement of the model based on 2815 observed reflections converged to a final R_F = 12.2%. The isolation of **1** and **2** from reactions of $LnCl_3$ with $NaOCMe_3$ depends critically on how the initial reaction mixture is handled. **1** is also observed as a product from the reaction of $EuCl_3$ with 3 equiv of $NaOCMe_3$, although the yields vary drastically depending on isolation procedures.

Introduction

As part of our investigations of the alkoxide chemistry of yttrium and the lanthanide metals, we have studied the reactions of yttrium and lanthanide trihalides with $NaOCMe_3$ in a variety of stoichiometries.[2-4] Reactions of YCl_3 with 3 and 2 equiv of $NaOCMe_3$ form $Y_3(OCMe_3)_8Cl(THF)_2$ (**4**)[2] and $Y_3(OCMe_3)_7Cl_2(THF)_2$ (**5**),[3] respectively, in high yield (reactions 1 and 2). Both complexes have been fully characterized by X-ray crystallography which has revealed the analogous structures $Y_3(OR)_3(\mu\text{-}OR)_3(\mu_3\text{-}OR)(\mu_3\text{-}Cl)Z(THF)_2$ in which Z = OR for **4** and Cl for **5** (R = CMe_3). Although the terminal chloride ligand in **5** can be readily replaced with a *tert*-butoxide group to form **4** (eq 3),[3] attempts to replace the μ_3-chloride group in **4** were unsuccessful. Both the reaction of **4** with $NaOCMe_3$ and the reaction of 4 equiv of $NaOCMe_3$ with YCl_3 give insoluble products instead of $Y_3(OCMe_3)_9(THF)_2$. This latter halide-free complex can, however, be prepared via an alternative route involving the reaction of $Y_3(OCMe_3)_9(HOCMe_3)_2$, obtained from $Y[N(SiMe_3)_2]_3$ and *tert*-butyl alcohol, with THF.[5]

$$YCl_3 + 3NaOCMe_3 \xrightarrow{80\%\ \text{yield}} \underset{\mathbf{4}}{Y_3(OCMe_3)_8Cl(THF)_2} + NaCl \quad (1)$$

$$YCl_3 + 2NaOCMe_3 \xrightarrow{75\%\ \text{yield}} \underset{\mathbf{5}}{Y_3(OCMe_3)_7Cl_2(THF)_2} + NaCl \quad (2)$$

$$\underset{\mathbf{5}}{Y_3(OCMe_3)_7Cl_2(THF)_2} + NaOCMe_3 \xrightarrow{80\%\ \text{yield}} \underset{\mathbf{4}}{Y_3(OCMe_3)_8Cl(THF)_2} + NaCl \quad (3)$$

We now report that although the reaction of **4** with $NaOCMe_3$ and the reaction of YCl_3 with 4 equiv of $NaOCMe_3$ give insoluble products, the reaction of YCl_3 with a large excess of $NaOCMe_3$ (10 equiv) gives a soluble yttrium *tert*-butoxide product. This product is a mixed metal complex which appears to be representative of a new general class of yttrium and lanthanide alkoxide materials of formula $LnNa_8(OR)_{10}X$. For Ln = Y, complexes with both X = Cl and OH have been characterized.

In contrast to the yttrium reaction 1, when the larger metal, lanthanum, is used, $La_3(OCMe_3)_9(THF)_2$ (**6**) is formed directly

(1) (a) University of California, Irvine. (b) Unocal Corporation.
(2) Evans, W. J.; Sollberger, M. S.; Hanusa, T. P. *J. Am. Chem. Soc.* **1988**, *110*, 1841–1850.
(3) Evans, W. J.; Sollberger, M. S. *Inorg. Chem.* **1988**, *27*, 4417–4423.
(4) Evans, W. J.; Olofson, J. M.; Ziller, J. W. *J. Am. Chem. Soc.* **1990**, *112*, 2308–2314.
(5) Bradley, D. C.; Chudzynska, H.; Hursthouse, M. B.; Motevalli, M. *Polyhedron* **1991**, *10*, 1049–1059.

0002-7863/93/1515-4120$04.00/0

Table I. Crystallographic Data for $EuNa_8(OCMe_3)_{10}Cl$ (**1**), $YNa_8(OCMe_3)_{10}Cl$ (**2**), and $YNa_8(OCMe_3)_{10}OH$ (**3**)

complex	**1**	**2**	**3**
formula	$C_{40}H_{90}O_{10}Na_8ClEu$	$C_{40}H_{90}O_{10}Na_8ClY$	$C_{40}H_{91}O_{11}Na_8Y$
F_w	1102.5	1039.4	1021.0
temp (K)	203	203	295
space group	*Pbca*	*Pbca*	*Pbca* [D_{2h}^{15}; No. 61]
a (Å)	20.395(4)	20.270(3)	20.423(3)
b (Å)	27.506(5)	27.332(4)	27.370(5)
c (Å)	21.496(4)	21.409(3)	21.633(4)
V (Å^3)	12,059(4)	11,861(3)	12,092(4)
Z	8	8	8
D_{calcd} (g/cm^3)	1.21	1.16	1.12
radiation	Mo Kα (λ = 0.71073 Å)	Mo Kα (λ = 0.71073 Å)	Mo Kα (λ = 0.71073 Å)
μ(Mo Kα) (mm^{-1})	1.182	1.131	1.07
trans coeff (min/max)	0.5104/0.5739	0.5083/0.6423	0.3844/0.4301
R_F (%); R_{wF} (%)[a]	6.4%; 7.3%	8.9%; 8.5%	12.2%; 13.1%

[a] $R_F = 100[\sum||F_o| - |F_c||/\sum|F_o|]$; $R_{wF} = 100[\sum w(|F_o| - |F_c|)^2/\sum w|F_o|^2]$.

from $LaCl_3$ and 3 equiv of $NaOCMe_3$ (eq 4).[2] As in the related

$$LaCl_3 + 3NaOCMe_3 \xrightarrow{85\%\ \text{yield}} La_3(OCMe_3)_9(THF)_2 + NaCl \quad (4)$$
6

yttrium system, a *tert*-butyl alcohol derivative of **6**, $La_3(OCMe_3)_9(HOCMe_3)_2$, can be prepared from $La[N(SiMe_3)_2]_3$ and *tert*-butyl alcohol. This complex has been crystallographically characterized and has the same basic structure as **4** and **5**.[5] However, lanthanum analogs of **4** and **5** have not been isolated.

To determine how a metal which is intermediate in size between yttrium and lanthanum compares in its reactivity with $NaOCMe_3$, the reactions of $EuCl_3$ with various amounts of $NaOCMe_3$ have been examined. The reactions of $EuCl_3$ with 3 and 10 equiv of $NaOCMe_3$ show similarities to the other metal systems in that trimetallic and nonametallic products appear to form, but the chemistry is much more complicated. In the europium reactions, mixtures of products can result whose composition depends critically on the specific isolation techniques employed. The isolation methods are so critical that with certain procedures $EuNa_8(OR)_{10}Cl$ can be isolated from a 3-equiv $NaOCMe_3$ reaction but not from a 10-equiv reaction! We report here on the details of these yttrium and europium reactions and the structures obtained.

Experimental Section

All of the complexes described below were handled with rigorous exclusion of air and water using Schlenk, vacuum line, and glovebox (Vacuum/Atmospheres) techniques. Physical measurements and purification of reagents have been described previously.[2-4] Complete elemental analytical data were obtained at Unocal.

$EuNa_8(\mu_3\text{-}OCMe_3)_8(\mu_4\text{-}OCMe_3)(OCMe_3)(\mu_x\text{-}Cl)$ (1). In the glovebox, $NaOCMe_3$ (344 mg, 3.6 mmol) was dissolved completely in 3 mL of THF and added to a stirred suspension of $EuCl_3$ (92 mg, 0.36 mmol) in 14 mL of THF. The bulk of the $EuCl_3$ suspension disappeared within 15 min. After the mixture was stirred overnight, the solvent was removed by rotary evaporation leaving an oily residue. Hexane (5 mL) was added to the residue which was then stirred for a period of 20 min. After removal of the hexane by rotary evaporation, the solid was treated with another 5-mL portion of hexane. Removal of the second hexane portion by rotary evaporation left a dry free-flowing powder. This solid was extracted with 10 mL of toluene and centrifuged to remove an insoluble component. Rotary evaporation of the toluene solution left **1** as a colorless crystalline solid (354 mg, 90% yield). **1** sublimes at 125 °C and 10^{-3} Torr. Anal. Calcd for $EuNa_8ClC_{40}H_{90}O_{10}$: Eu, 13.78; Na, 16.68; Cl, 3.22; C, 43.58; H, 8.23. Found: Eu, 15.1; Na, 16.2; Cl, 3.3; C, 44.0; H, 8.1. Reactions run for shorter reaction times gave the same product.

$YNa_8(\mu_3\text{-}OCMe_3)_8(\mu_4\text{-}OCMe_3)(OCMe_3)(\mu_x\text{-}Cl)$ (2). Following the procedure above for **1**, $NaOCMe_3$ (1.058 g, 11 mmol) was reacted with YCl_3 (215 mg, 1.1 mmol) to form **2** as a colorless crystalline solid (966 mg, 84%). **2** sublimes at 125 °C and 10^{-3} Torr. Anal. Calcd for $YNa_8ClC_{40}H_{90}O_{10}$: Y, 8.55; Na, 17.69; Cl, 3.41. Found: Y, 7.95; Na, 17.9; Cl, 5.1.

$YNa_8(\mu_3\text{-}OCMe_3)_8(\mu_4\text{-}OCMe_3)(OCMe_3)(\mu_x\text{-}OH)$ (3). Following the general procedure described above for the preparation of **1** and **2**, complex **3** was isolated from a reaction between YCl_3 and $NaOCMe_3$ which had not been sublimed prior to use to remove impurities such as NaOH. Complex **3** was isolated as a trace crystalline product from a mixture which contained no other components identifiable by NMR spectroscopy.

X-ray Data Collection, Structure Determination, and Refinement for $YNa_8(\mu_3\text{-}OCMe_3)_8(\mu_4\text{-}OCMe_3)(OCMe_3)(\mu_x\text{-}OH)$ (3). A colorless crystal of approximate dimensions 0.23 × 0.43 × 0.53 mm was mounted in a thin-walled glass capillary under an inert (N_2) atmosphere and accurately aligned on a Siemens P3 automated diffractometer. Subsequent setup operations (determination of accurate unit cell dimensions and orientation matrix) and collection of room temperature (295 K) intensity data were carried out using standard techniques similar to those of Churchill.[6] Experimental details are given in Table I.

All 7950 data were corrected for the effects of absorption and for Lorentz and polarization effects and placed on an approximately absolute scale. A careful survey of the data set revealed the systematic extinctions $0kl$ for $l = 2n + 1$, $h0l$ for $h = 2n + 1$, and $hk0$ for $k = 2n + 1$; the diffraction symmetry was mmm. This is consistent with space group *Pcab*, a nonstandard setting of the centrosymmetric orthorhombic space group *Pbca* [D_{2h}^{15}; No. 61]. A transformation was done to convert the space group to the standard setting, *Pbca*; all final parameters are based on this setting.

All crystallographic calculations were carried out using either our locally modified version of the UCLA Crystallographic Computing Package[7] or the SHELXTL PLUS program set.[8] The analytical scattering factors for neutral atoms were used throughout the analysis;[9a] both the real ($\Delta f'$) and imaginary ($i\Delta f''$) components of anomalous dispersion[9b] were included. The quantity minimized during least-squares analysis was $\sum w(|F_o| - |F_c|)^2$ where $w^{-1} = \sigma^2(|F_o|) + 0.0011(|F_o|)^2$.

The structure was solved by direct methods (MITHRIL)[10] and refined by full-matrix least-squares techniques. Hydrogen atom contributions were included using a riding model with d(C–H) = 0.96 Å and U(iso) = 0.10 Å^2. Refinement of positional and thermal parameters (anisotropic for O, Na, Y) led to convergence with R_F = 12.2%, R_{wF} = 13.1%, and GOF = 2.36 for 341 variables refined against those 2815 data with $|F_o| > 4.0\sigma(|F_o|)$. A final difference-Fourier synthesis was devoid of significant features, ρ(max) = 0.97 e Å^{-3}.

X-ray Data Collection, Structure Determination, and Refinement for $YNa_8(\mu_3\text{-}OCMe_3)_8(\mu_4\text{-}OCMe_3)(OCMe_3)(\mu_x\text{-}Cl)$ (2). A colorless crystal of approximate dimensions 0.50 × 0.53 × 0.57 mm was immersed in Paratone-N oil, mounted on a glass fiber, and transferred to the Syntex $P2_1$ diffractometer which is equipped with a UCI-modified LT-1 apparatus. The crystal was examined at 203 K by procedures described above for **3** (see Table I). The 10508 data were handled as described above for **3**. The quantity minimized during least-squares analysis was

(6) Churchill, M. R.; Lashewycz, R. A.; Rotella, F. J. *Inorg. Chem.* **1977**, *16*, 265–271.
(7) UCLA Crystallographic Computing Package; University of California, Los Angeles, 1981, C. Strouse, personal communication.
(8) Siemens Analytical X-ray Instruments, Inc.; Madison, Wisconsin, 1989.
(9) International Tables for X-ray Crystallography; Kynoch Press: Birmingham, England, 1974; (a) pp 99–101; (b) pp 149–150.
(10) Gilmore, C. J. *J. Appl. Crystallogr.* **1984**, *17*, 4246.

Table II. ^{1}H NMR Data for Complexes **1–3**

complex	solvent	chemical shift (ppm)
$EuNa_8(OR)_{10}Cl$ (**1**)	benzene-d_6	12.12 (s, 9H), 4.21 (s, 9H), 1.94 (s, 36H), –6.00 (s, 36H)
$YNa_8(OR)_{10}Cl$ (**2**)	benzene-d_6	1.61 (s, 9H), 1.44 (s, 36H), 1.21 (s, 45H)
	THF-d_8	1.54 (s, 9H), 1.24 (s, 36H), 1.10 (s, 45H)
$YNa_8(OR)_{10}(OH)$ (**3**)	benzene-d_6	1.72 (s, 9H), 1.54 (s, 36H), 1.19 (s, 45H)
	THF-d_8	1.26 (br), 1.06 (br) (1:3)

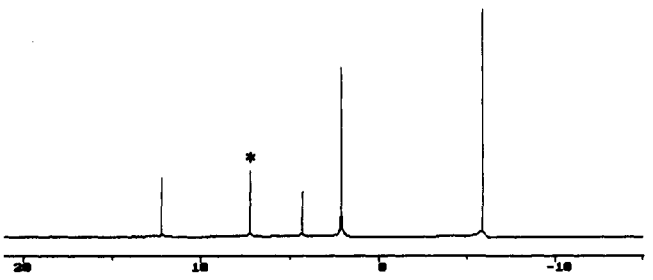

Figure 1. ^{1}H NMR spectrum of $EuNa_8(OCMe_3)_{10}Cl$ (**1**) in benzene-d_6. The solvent peak is indicated by an asterisk.

$\sum w(|F_o| - |F_c|)^2$ where $w^{-1} = \sigma^2(|F_o|) + 0.003(|F_o|)^2$. The coordinates of the $YNa_8O_{10}C_{10}$ core of **3** were used to successfully phase the present model. Subsequent difference-Fourier syntheses revealed the positions of the chlorine and remaining carbon atoms. Refinement of positional and anisotropic thermal parameters led to convergence with $R_F = 8.9\%$, $R_{wF} = 8.5\%$, and GOF = 1.89 for 536 variables refined against those 4876 data with $|F_o| > 4.0\sigma(|F_o|)$. Hydrogen atom contributions were included using a riding model with d(C–H) = 0.96 Å and U(iso) = 0.10 Å^2. A final difference-Fourier synthesis showed no significant features, ρ(max) = 0.81 e Å^{-3}.

X-ray Data Collection, Structure Determination, and Refinement for $EuNa_8(\mu_3\text{-}OCMe_3)_8(\mu_4\text{-}OCMe_3)(OCMe_3)(\mu_x\text{-}Cl)$ (1). A colorless crystal of approximate dimensions 0.23 × 0.30 × 0.50 mm was handled as described above for **2** (see Table I). The 7917 data were handled as described above for **2**. The quantity minimized during least-squares analysis was $\sum w(|F_o| - |F_c|)^2$ where $w^{-1} = \sigma^2(|F_o|) + 0.001(|F_o|)^2$. The coordinates of **2** were used to successfully phase the present model. Refinement of positional and anisotropic thermal parameters led to convergence with $R_F = 6.4\%$, $R_{wF} = 7.3\%$, and GOF = 1.46 for 536 variables refined against those 4844 data with $|F_o| > 4.0\sigma(|F_o|)$. Hydrogen atom contributions were included using a riding model with d(C–H) = 0.96 Å and U(iso) = 0.10 Å^2. A final difference-Fourier synthesis showed no significant features, ρ(max) = 0.95 e Å^{-3}.

Results

Synthesis of $EuNa_8(OCMe_3)_{10}Cl$ (1) and $YNa_8(OCMe_3)_{10}Cl$ (2). Both $EuCl_3$ and YCl_3 react with 10 equiv of $NaOCMe_3$ in THF to give a single primary product which can be isolated in 80–90% yield. To obtain these high yields, however, requires a product isolation procedure which includes removal of THF, washing with hexane, and extraction with toluene. Other isolation procedures have given only trace quantities of **1** and **2**. The ^{1}H NMR spectrum of diamagnetic **2** (Table II) in THF-d_8 or benzene-d_6 consists of three resonances which integrate in a ratio of 1:4:5. This suggested the presence of at least ten alkoxide groups in the product. The ^{1}H NMR spectrum of paramagnetic **1** in benzene-d_6 (Figure 1) similarly contained resonances for ten alkoxide groups. In this case, four distinct resonances were observed in a 1:1:4:4 pattern and in a shift range of 12 to –6 ppm. To our knowledge this is the first ^{1}H NMR data on any europium alkoxide complexes. Complete elemental analysis on both complexes indicated the presence of sodium and chloride, in addition to the lanthanide element, and an overall Ln:Na:Cl ratio of 1:8:1 was found. Single-crystal X-ray diffraction studies revealed a structure for **1** and **2** which was entirely consistent with these data (Figures 2 and 3). The equation for the formation of **1** and **2** is given in eq 5.

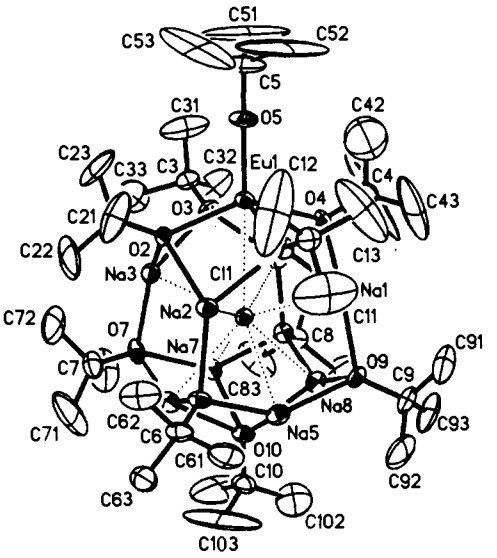

Figure 2. ORTEP diagram of $EuNa_8(OCMe_3)_{10}Cl$ (**1**) with thermal ellipsoids drawn at the 20% probability level.

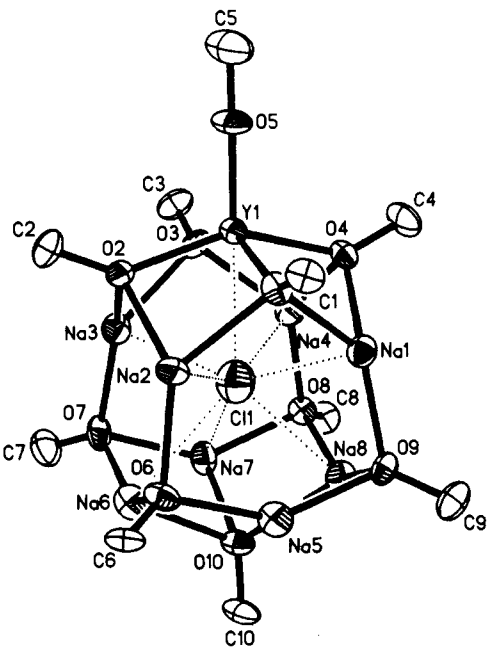

Figure 3. ORTEP diagram of $YNa_8(OCMe_3)_{10}Cl$ (**2**) with methyl groups deleted for clarity. The thermal ellipsoids are drawn at the 30% probability level.

$$LnCl_3 + 10NaOCMe_3 \rightarrow LnNa_8(OCMe_3)_{10}Cl + 2NaCl \quad (5)$$

Isolation of $YNa_8(OCMe_3)_{10}(OH)$. In one of the reactions of YCl_3 with $NaOCMe_3$, a crystalline product, **3**, which had a ^{1}H NMR spectrum slightly different from complex **2**, was isolated. Although the pattern of resonances for **3** in benzene-d_6 matched that for complex **2**, the chemical shifts for the three peaks were not the same. In addition, the ^{1}H NMR spectrum of **3** in THF-d_8 was completely different from that for complex **2**, exhibiting only two peaks in a ratio of 1:3 (Table II).

X-ray crystallography was used to establish the identity of **3** (Figure 4). Complex **3** is structurally similar to **1** and **2** except that a hydroxide ligand occupies the central position occupied by a chloride group in the other complexes. The hydroxide in this particular product is likely to have been introduced as a contaminant in the $NaOCMe_3$ reagent used. Although we have not attempted to repeat the synthesis of this material, the isolation

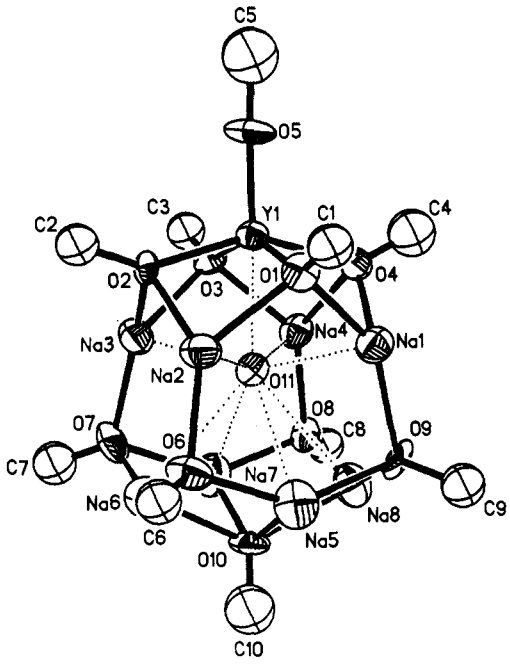

Figure 4. ORTEP diagram of $YNa_8(OCMe_3)_{10}(OH)$ (**3**) with methyl groups deleted for clarity. Thermal ellipsoids are drawn at the 40% probability level.

of this complex illustrates the generality of this nonametallic structural class.

X-ray Crystal Structures of 1–3. Figures 2–4 and Tables III and IV present the crystallographic data obtained on **1–3**. The room temperature structure of **3** did not give as good a data set as was obtained at low temperature for **1** and **2** and, hence, the specific bond distances for this structure are less reliable. In addition, the hydroxide hydrogen atom was not located.

The nine metals in **1–3** occupy the vertices of a capped square antiprism with the single europium or yttrium atom in the unique capping position. This nonametallic unit is held together by two distinct sets of four triply-bridging alkoxide ligands, one quadruply-bridging alkoxide, and a centralized chloride or hydroxide ligand. The remaining alkoxide is located in a terminal position attached to the lanthanide atom. In one set of four μ_3-alkoxide ligands, each μ_3-alkoxide spans one of the four triangular $LnNa_2$ faces of the $LnNa_4$ square pyramidal unit which comprises the top of the structure (Ln(1) and Na(1)–Na(4)) as shown in the figures. In the second set of four μ_3-alkoxide ligands, each alkoxide is connected to one sodium atom in the top Na_4 plane and two sodium atoms in the bottom Na_4 plane (Na(5)–Na(8)). The μ_4-alkoxide occupies a position in which it interacts with all four sodium atoms in the bottom Na_4 plane. The central ligand is located inside the $LnNa_8$ cavity between the top and bottom Na_4 planes. The lanthanide atoms in **1–3** are formally bound to four triply-bridging alkoxide groups and a single terminal alkoxide. Their coordination number is five or six depending upon how the interaction with the central ligand is defined. Six-coordination is most commonly found in lanthanide *tert*-butoxide complexes.[2-5,11] The sodium atoms of the upper pentametallic $LnNa_4$ subunit are four-coordinate, while those of the Na_4 square at the bottom of the structures are three- or four-coordinate again depending on how the bonding interaction with the chloride ligand is defined.

The square antiprismatic arrangement of the eight sodium atoms in each of the structures is very regular. In all three complexes, the top Na_4 subunits are planar to 0.005 Å and the bottom Na_4 subunits are planar to 0.03 Å. The distances between the two Na_4 planes are nearly coincident in the three structures:

(11) Evans, W. J.; Deming, T. J.; Olofson, J. M.; Ziller, J. W. *Inorg. Chem.* **1989**, *28*, 4027–4034.

Table III. Selected Bond Distances (Å) for $EuNa_8(OCMe_3)_{10}Cl$ (**1**), $YNa_8(OCMe_3)_{10}Cl$ (**2**), and $YNa_8(OCMe_3)_{10}(OH)$ (**3**)

complex		1	2	3
Ln–Cl[a]	Ln(1)–Cl(1)	3.105(3)	2.915(4)	2.631(13)[a]
Ln–$OCMe_3$	Ln(1)–O(5)	2.090(8)	2.044(7)	2.022(16)
Ln–μ_3-$OCMe_3$	Ln(1)–O(1)	2.326(7)	2.275(6)	2.280(14)
	Ln(1)–O(2)	2.332(7)	2.284(6)	2.263(13)
	Ln(1)–O(3)	2.339(7)	2.287(6)	2.274(14)
	Ln(1)–O(4)	2.343(7)	2.286(6)	2.291(14)
Na–Cl[a]	Na(1)–Cl(1)	2.744(5)	2.670(5)	2.517(16)[a]
	Na(2)–Cl(1)	2.746(5)	2.661(5)	2.533(16)[a]
	Na(3)–Cl(1)	2.731(5)	2.644(5)	2.535(16)[a]
	Na(4)–Cl(1)	2.743(5)	2.642(5)	2.517(16)[a]
	Na(5)–Cl(1)	2.869(5)	2.930(5)	
	Na(6)–Cl(1)	2.901(5)	2.991(5)	
	Na(7)–Cl(1)	2.895(5)	2.960(5)	
	Na(8)–Cl(1)	2.920(5)	3.032(5)	
Na–μ_3-$OCMe_3$	Na(1)–O(1)	2.381(8)	2.340(7)	2.342(15)
	Na(2)–O(1)	2.347(8)	2.342(7)	2.320(16)
	Na(2)–O(2)	2.339(8)	2.322(7)	2.290(16)
	Na(3)–O(2)	2.368(8)	2.356(7)	2.346(16)
	Na(3)–O(3)	2.364(8)	2.331(7)	2.319(17)
	Na(4)–O(3)	2.374(8)	2.334(7)	2.311(16)
	Na(1)–O(4)	2.342(9)	2.322(8)	2.314(18)
	Na(4)–O(4)	2.372(8)	2.344(7)	2.301(17)
	Na(2)–O(6)	2.265(9)	2.241(7)	2.236(18)
	Na(5)–O(6)	2.279(9)	2.249(8)	2.222(18)
	Na(6)–O(6)	2.286(9)	2.261(8)	2.217(19)
	Na(3)–O(7)	2.259(9)	2.231(7)	2.232(17)
	Na(6)–O(7)	2.290(10)	2.260(8)	2.262(20)
	Na(7)–O(7)	2.258(9)	2.252(7)	2.236(18)
	Na(4)–O(8)	2.257(8)	2.247(7)	2.274(15)
	Na(7)–O(8)	2.269(8)	2.257(7)	2.220(17)
	Na(8)–O(8)	2.258(8)	2.245(7)	2.184(17)
	Na(1)–O(9)	2.252(9)	2.251(7)	2.226(17)
	Na(5)–O(9)	2.276(9)	2.253(8)	2.221(19)
	Na(8)–O(9)	2.264(9)	2.235(7)	2.215(18)
Na–μ_4-$OCMe_3$	Na(5)–O(10)	2.374(9)	2.369(7)	2.368(18)
	Na(6)–O(10)	2.380(9)	2.362(7)	2.348(17)
	Na(7)–O(10)	2.376(9)	2.348(7)	2.320(19)
	Na(8)–O(10)	2.388(9)	2.376(8)	2.420(18)

[a] For complex **3**, these are Ln–O(11) and Na–O(11) distances of the internal hydroxide ligand.

2.95, 2.94, and 2.95 Å for **1–3**, respectively. The fully staggered arrangement of the two Na_4 units in **1** is shown in Figure 5.

The position of the internal ligand in **1–3** between the two Na_4 planes varies from structure to structure. In all cases, it is closer to the top Na_4 plane, i.e., the pentametallic $LnNa_4$ subunit, than to the bottom Na_4 plane. The distances to the top and to the bottom Na_4 planes respectively are 0.93 and 2.02 Å for **1**, 0.82 and 2.12 Å for **2**, and 0.56 and 2.39 Å for **3**. Hence, the internal chloride is furthest from the lanthanide in the europium complex and the internal ligand closest to the lanthanide is the hydroxide oxygen atom in **3**. The relative position of this internal atom appears to affect other distances in these complexes as described below.

Specific bond distances for yttrium will be described first since there are more data in the literature for comparison with this metal. The terminal Y–O($OCMe_3$) distances of 2.044(7) and 2.022(16) Å for **2** and **3**, respectively, are normal and fall within the range of terminal Y–O($OCMe_3$) distances previously observed for yttrium alkoxide complexes, 1.97(2)–2.07(2) Å.[2-4] The Y–O(μ_3-$OCMe_3$) distances of 2.275(6)–2.287(6) and 2.263(13)–2.291(14) Å for **2** and **3**, respectively, are near the low end of the range of analogous distances observed previously for complexes in which only yttrium atoms are involved in the bonding, 2.306(8)–2.556(13) Å.[2-4] The 2.915(4) Å Y–Cl distance in **2** is the longest observed for a Y–Cl interaction,[12,13] but it is only slightly longer than the upper end of the 2.820(5)–2.897(6) Å range of

(12) Evans, W. J.; Foster, S. E. *J. Organomet. Chem.* **1992**, *433*, 79–94.
(13) Evans, W. J.; Peterson, T. T.; Rausch, M. D.; Hunter, W. E.; Zhang, H.; Atwood, J. L. *Organometallics* **1985**, *4*, 554–559.

Table IV. Selected Interatomic Angles (deg) in $EuNa_8(OCMe_3)_{10}Cl$ (**1**), $YNa_8(OCMe_3)_{10}Cl$ (**2**), and $YNa_8(OCMe_3)_{10}(OH)$ (**3**)[a]

complex	1	2	3
Cl(1)–Ln(1)–O(1)	71.8(2)	73.9(2)	74.5(4)
Cl(1)–Ln(1)–O(2)	71.9(2)	74.1(2)	74.7(4)
Cl(1)–Ln(1)–O(3)	71.5(2)	73.0(2)	74.6(4)
Cl(1)–Ln(1)–O(4)	71.7(2)	73.9(2)	74.4(5)
O(2)–Ln(1)–O(3)	84.3(2)	84.9(2)	86.6(5)
O(1)–Ln(1)–O(2)	84.3(2)	86.0(2)	85.5(5)
O(1)–Ln(1)–O(4)	84.6(3)	85.9(2)	86.6(5)
O(3)–Ln(1)–O(4)	84.3(3)	85.3(2)	85.1(5)
O(1)–Ln(1)–O(5)	108.6(3)	105.6(3)	105.4(6)
O(2)–Ln(1)–O(5)	107.1(3)	105.5(2)	104.5(6)
O(3)–Ln(1)–O(5)	108.0(3)	107.4(3)	105.4(6)
O(4)–Ln(1)–O(5)	109.2(3)	106.5(3)	106.4(6)
O(1)–Ln(1)–O(3)	143.3(2)	146.9(2)	149.2(5)
O(2)–Ln(1)–O(4)	143.7(2)	148.0(2)	149.1(5)
Cl(1)–Ln(1)–O(5)	179.0(2)	179.5(2)	179.2(6)
Ln(1)–O(5)–C(5)	178.8(10)	177.4(8)	176.3(21)
Cl(1)–Na(1)–O(1)	78.3(2)	78.0(2)	75.7(5)
Cl(1)–Na(1)–O(4)	79.0(2)	78.3(2)	76.3(6)
Cl(1)–Na(1)–O(9)	81.8(2)	83.4(2)	88.9(6)
Cl(1)–Na(2)–O(1)	78.8(2)	78.1(2)	75.8(5)
Cl(1)–Na(2)–O(2)	79.1(2)	78.8(2)	76.3(5)
Cl(1)–Na(2)–O(6)	81.7(2)	84.0(2)	89.0(6)
Cl(1)–Na(3)–O(2)	78.9(2)	78.6(2)	75.3(5)
Cl(1)–Na(3)–O(3)	78.6(2)	77.8(2)	75.8(5)
Cl(1)–Na(3)–O(7)	82.2(2)	84.8(2)	91.3(6)
Cl(1)–Na(4)–O(3)	78.2(2)	77.8(2)	76.3(5)
Cl(1)–Na(4)–O(4)	78.6(2)	78.5(2)	76.5(5)
Cl(1)–Na(4)–O(8)	82.1(2)	84.7(2)	89.5(5)
Cl(1)–Na(5)–O(6)	78.7(2)	77.7(2)	75.9(6)
Cl(1)–Na(5)–O(9)	78.7(2)	77.6(2)	75.4(5)
Cl(1)–Na(5)–O(10)	74.3(2)	74.1(2)	76.5(5)
Cl(1)–Na(6)–O(6)	77.9(2)	76.3(2)	73.4(5)
Cl(1)–Na(6)–O(7)	77.9(2)	76.5(2)	74.7(5)
Cl(1)–Na(6)–O(10)	73.6(2)	73.0(2)	74.3(5)
Cl(1)–Na(7)–O(7)	78.5(2)	77.3(2)	73.7(5)
Cl(1)–Na(7)–O(8)	78.5(2)	77.3(2)	74.8(5)
Cl(1)–Na(7)–O(10)	73.7(2)	73.8(2)	75.2(5)
Cl(1)–Na(8)–O(8)	78.1(2)	75.9(2)	74.0(5)
Cl(1)–Na(8)–O(9)	77.7(2)	75.6(2)	72.3(5)
Cl(1)–Na(8)–O(10)	73.1(2)	72.1(2)	72.9(5)
O(1)–Na(1)–O(4)	83.4(3)	83.6(2)	84.6(6)
O(1)–Na(2)–O(2)	83.7(3)	83.6(2)	83.9(6)
O(2)–Na(3)–O(3)	83.0(3)	82.3(2)	83.6(5)
O(3)–Na(4)–O(4)	82.9(3)	82.9(2)	84.0(5)
O(1)–Na(1)–O(9)	132.5(3)	133.2(3)	134.1(7)
O(4)–Na(1)–O(9)	133.9(3)	133.9(3)	133.9(6)
O(1)–Na(2)–O(6)	133.3(3)	133.6(3)	134.9(7)
O(2)–Na(2)–O(6)	133.1(3)	134.2(3)	133.8(7)
O(2)–Na(3)–O(7)	135.5(3)	135.9(3)	135.6(7)
O(3)–Na(3)–O(7)	131.8(3)	133.4(3)	134.5(6)
O(3)–Na(4)–O(8)	134.1(3)	135.4(3)	135.0(7)
O(4)–Na(4)–O(8)	132.7(3)	133.2(3)	134.3(6)
O(6)–Na(5)–O(9)	143.0(3)	143.5(3)	142.9(7)
O(6)–Na(6)–O(7)	142.0(3)	140.2(3)	138.7(7)
O(7)–Na(7)–O(8)	141.5(3)	141.1(3)	139.7(7)
O(8)–Na(8)–O(9)	140.9(3)	138.6(3)	137.6(7)
O(6)–Na(5)–O(10)	100.9(3)	99.6(3)	97.1(7)
O(9)–Na(5)–O(10)	100.7(3)	99.0(3)	98.5(7)
O(6)–Na(6)–O(10)	100.5(3)	99.5(3)	97.9(7)
O(7)–Na(6)–O(10)	100.2(3)	99.7(3)	97.9(6)
O(7)–Na(7)–O(10)	101.3(3)	100.3(3)	99.5(7)
O(8)–Na(7)–O(10)	101.3(3)	100.3(3)	98.8(7)
O(8)–Na(8)–O(10)	101.2(3)	99.7(3)	96.8(6)
O(9)–Na(8)–O(10)	100.6(3)	99.3(3)	97.2(6)

[a] For complex **3** the Cl(1) label in the first column refers to the central oxygen atom O(11).

Y–Cl(μ_3-Cl) distances in $Y_3(OCMe_3)_8Cl(THF)_2$,[2] $Y_3(OCMe_3)_7Cl_2(THF)_2$,[3] and $Y_{14}(OCMe_3)_{28}Cl_{10}O_2(THF)_4$.[3]

Evaluation of the 2.631(13) Å Y–O(OH) distance in **3** is difficult because comparable analogs are not available. This Y–O distance is much longer than the Y–O(μ-OH) distances of 2.33-(2) and 2.36(2) Å in $[(C_5H_5)_2Y(\mu\text{-OH})]_2(C_6H_5C{\equiv}CC_6H_5)$,[14] which has an OH group which is only doubly-bridging. The Y–O distance in **3** is also longer than the 2.27(2)–2.41(2) Å Y–O(μ_5-O) distances found for the central oxides in $(C_5H_5)_5Y_5(\mu\text{-OMe})_4(\mu_3\text{-OMe})_4(\mu_5\text{-O})$[15] and $(Me_2HCO)_5Y_5(\mu\text{-OCHMe}_2)_4(\mu_3\text{-OCHMe}_2)_4(\mu_5\text{-O})$.[16-18] It is interesting to note that the latter pentametallic complexes have square pyramidal arrangements of atoms similar to the $LnNa_4$ subunit at the top of **1**–**3**.

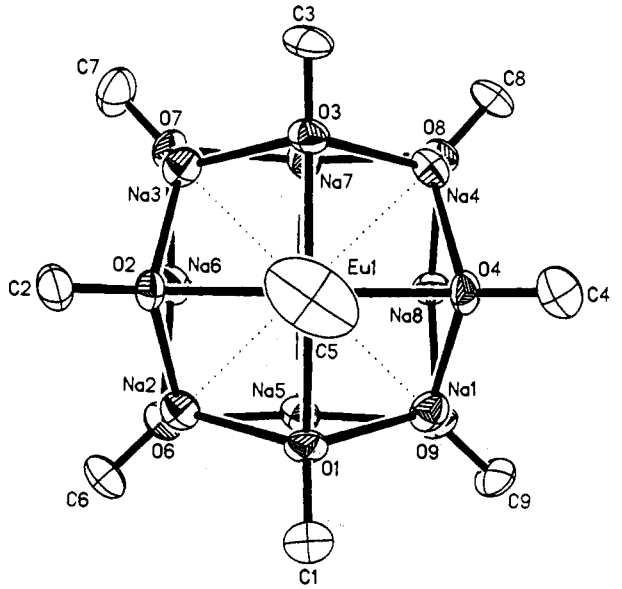

Figure 5. View of $EuNa_8(OCMe_3)_{10}Cl$ down the C(5)–O(5)–Eu–Cl vector to show the regularity of the square antiprismatic arrangement of sodium atoms (methyl groups deleted for clarity).

The Eu–O distances in **1** are larger than the Y–O distances in **2** and **3** by approximately the difference in the six-coordinate radii of these metals according to Shannon, i.e., 0.047 Å.[19] Hence, the terminal Eu–O(OR) distance is 2.090(8) Å and the bridging Eu–O(μ-OR) distances range from 2.326(7) to 2.343(7) Å. However, the Eu–Cl distance is 0.09 Å longer than the Y–Cl distance. This is consistent with the fact that the internal chloride is further from the top Na_4 plane in **1** than in **2**. The Na–Cl distances in **1** and **2** seem to respond to this difference in Ln–Cl distance between the two structures as described below.

In both **1** and **2**, the overall average Na–Cl distance is 2.82(13) Å, a distance that is coincident with the 2.814-Å Na–Cl distance in NaCl.[20] However, in both structures this average is comprised of two distinct sets of Na–Cl distances. In both complexes, a shorter set of Na–Cl distances is found for the sodium atoms closest to the lanthanide, i.e., Na(1)–Na(4), than for the other sodium atoms, Na(5)–Na(8). The Cl–Na(1–4) average distance is 2.74(1) Å in **1** and 2.65(1) Å in **2**. The Cl–Na(5–8) average distance is 2.90(2) Å in **1** and 2.98(4) Å in **2**. Hence, the internal chloride is more closely associated with the upper set of four sodium atoms. This is reasonable since this internal atom is also associated with the lanthanide above the upper Na_4 square. A similar situation is observed in **3**. The O(OH)–Na(1–4) average distance, 2.53(1) Å, is shorter than the O(OH)–Na(5–8) distances

(14) Evans, W. J.; Hozbor, M. A.; Bott, S. G.; Atwood, J. L. *Inorg. Chem.* **1988**, *27*, 1990–1993.
(15) Evans, W. J.; Sollberger, M. S. *J. Am. Chem. Soc.* **1986**, *108*, 6095–6096.
(16) Poncelet, O.; Sartain, W. J.; Hubert-Pfalzgraf, L. G.; Folting, K.; Caulton, K. G. *Inorg. Chem.* **1989**, *28*, 263–267.
(17) Bradley, D. C.; Chudzynska, H.; Frigo, D. M.; Hursthouse, M. B.; Mazid, M. A. *J. Chem. Soc., Chem. Commun.* **1988**, 1258–1259.
(18) Bradley, D. C.; Chudzynska, H.; Frigo, D. M.; Hammond, M. E.; Hursthouse, M. B.; Mazid, M. A. *Polyhedron* **1990**, *9*, 719–726.
(19) Shannon, R. D. *Acta Crystallorg.* **1976**, *A32*, 751–767.
(20) Wells, A. F. *Structural Inorganic Chemistry*; Clarenden Press: Oxford, 1975; p 375.

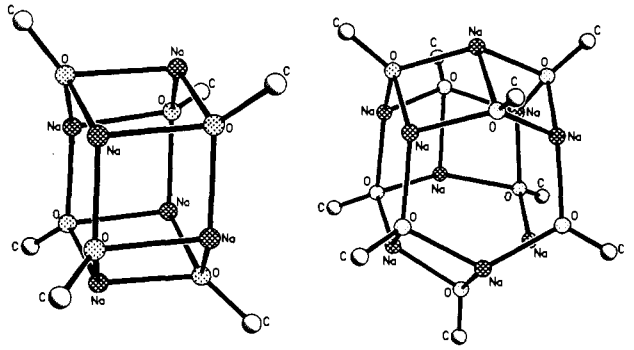

Figure 6. The $[(NaOCMe_3)_6]$ and $[(NaOCMe_3)_9]$ components of the structure of $NaOCMe_3$ with methyl groups omitted for clarity. The molecular structure of $(NaOCMe_3)_9$ is in an orientation suitable for comparison with **1–3**. The sodium atom at the top and the two sodium atoms at the bottom are in the capping positions of the tricapped trigonal prism generated by the nine sodium atoms.

which are all longer than 3.10 Å. This suggests that the hydroxide hydrogen atom is located in the lower region of this complex.

Comparison of the Na–Cl distances in the europium complex versus those in the yttrium complex is also valuable. The Cl–Na(1–4) distances in **2** are shorter than those in **1**, which is consistent with the fact that the Y–Cl distance in **2** is shorter than the Eu–Cl distance in **1**. Hence, the chloride in **2** is more involved in the upper part of the structure. This may be important in the overall stability of **2** versus **1** in solution (see below).

Like the Na–Cl distances, the Na–O(μ_3-$OCMe_3$) bond lengths in **1** and **2** also fall into two distinct ranges. In **1**, the Na–O distances in the top part of the molecule, which involve O(1)–O(4) and Ln–O–Na_2 units, range from 2.339(8) to 2.381(8) Å and average 2.36(2) Å. In contrast, the Na–O(μ_3-$OCMe_3$) distances in the bottom part of the molecule, which involve O(6)–O(9) and Na–O–Na_2 units, range from 2.252(9) to 2.290(10) Å and average 2.263 Å. The same trend is found in **2** except that the Na–O distances are 0.02–0.03 Å smaller in the yttrium complex. Hence, short Na–O distances are found for sodium atoms with long Na–Cl distances and vice versa.

The Na–O(μ_3-$OCMe_3$) distances in **1** and **2** can be compared with the Na–O(μ_3-$OCMe_3$) distances in $NaOCMe_3$. As shown in Figure 6, $NaOCMe_3$ crystallizes with a nonameric and a hexameric molecule in the asymmetric unit, i.e., as $[(NaOCMe_3)_9]$-$[(NaOCMe_3)_6]$.[21] In both components, the sodium atoms are three-coordinate and there are only triply-bridging alkoxide ligands. Nonameric $(NaOCMe_3)_9$ is actually very closely related structurally to **1–3** (see Discussion Section). In $(NaOCMe_3)_9$ and $(NaOCMe_3)_6$, the Na–O(μ_3-$OCMe_3$) distances range from 2.191(18) to 2.501(16) and 2.176(17) to 2.335(16) Å, respectively. This large range spans the spread of Na–O(μ_3-$OCMe_3$) distances in **1** and **2**.

As expected, the Na–O(μ_4-$OCMe_3$) distances in **1** and **2** (average 2.380 and 2.364 Å, respectively; range 2.376(8)–2.348(7) Å) are the longest Na–O lengths in these structures. However, these distances still fall within the range of Na–O bond lengths observed for the structures of $NaOCMe_3$, despite the difference in coordination. It is of interest to note that these distances are also only slightly longer than the Na–O(μ_3-$OCMe_3$) distances involving the Ln–O units in **1** and **2**.

Both **1** and **2** are quite regular in geometry as shown by the angular data in Table IV. Sets of analogous angles show only a small range of variation. For example, the O–Ln–O angles at the top of the structure (i.e., O(5)–Ln–O(1–4)) vary only from 107.1(3)° to 109.2(3)°. Numerous sets of similar angles are evident in Table IV. The other angle of note is the Ln–O–C angle of the single terminal *tert*-butoxide ligand. In both **1** and **2** this is nearly linear: 178.8(10)° in **1** and 177.4(8)° in **2**.

(21) Greiser, T.; Weiss, E. *Chem. Ber.* **1977**, *110*, 3388–3396.

NMR Spectroscopy. The 1:1:4:4 pattern of resonances in the ^1H NMR spectrum of complex **1** in benzene-d_6 (Figure 1) is entirely consistent with the solid-state structure. Although definitive assignments for these resonances cannot be made, it is likely that the most shifted resonances are due to the ligands nearest the paramagnetic europium center. Hence, the furthest downfield resonance (12.12 ppm) which integrates for one alkoxide group is likely to arise from the terminal *tert*-butoxide and the area 4 resonance at –6.00 ppm is likely to be due to the μ_3-alkoxide ligands bound to europium.

In the benzene-d_6 ^1H NMR spectrum of complexes **2** and **3**, only three of the four expected alkoxide resonances were observed. The three resonances, however, integrated in a ratio of 1:4:5, thus accounting for all ten alkoxide groups identified in the solid-state structures. The broadened area 5 resonance could not be resolved even at 500 MHz. It is uncertain if the area 1 resonance in these two complexes is due to the unique terminal *tert*-butoxide or the unique μ_4-*tert*-butoxide. Previously reported NMR spectra of yttrium *tert*-butoxide complexes have had the terminal alkoxide resonances at the highest field.[3] However, since $NaOCMe_3$ resonates upfield of the range of yttrium *tert*-butoxide resonances, the trends observed in pure yttrium *tert*-butoxide complexes may not be the same in these mixed-metal systems. The sensitivity of the shifts to environment can be seen from the fact that although complexes **2** and **3** exhibit identical resonance patterns in benzene-d_6, the chemical shifts for the two sets of resonances were different due to the different internal ligand. The hydroxide proton in complex **3** was not observed.

In contrast to the close correlation with structure observed for complex **1** in benzene-d_6, the ^1H NMR spectrum in THF-d_8 consisted of only a single broad alkoxide resonance. Furthermore, this NMR sample in THF-d_8, upon removal of the THF and redissolving in benzene-d_6, failed to reproduce the characteristic four-peak resonance pattern of **1**. In contrast, the ^1H NMR spectrum for **2** in THF-d_8 exhibited the same three-resonance pattern observed for this complex in benzene-d_6. The ^1H NMR for **3** in THF-d_8 was different from that for both complexes **1** and **2**, exhibiting two resonances which integrated in a ratio of 1:3!

These results suggest that only complex **2** is stable in solutions of THF. This is an interesting finding given the fact that complexes **1**, **2**, and **3** are isolated from a reaction which is originally conducted in THF. This presumably relates to the fact that removal of all THF in the product workup is necessary to ensure the formation of the lanthanide–sodium alkoxide structure (see next section). The single resonance in THF-d_8 for complex **1** could be due to the formation of free $NaOCMe_3$. If free $NaOCMe_3$ forms in solutions of **1** in THF, the resulting europium fragment, $Eu(OCMe_3)_{3-x}Cl_x(THF)$ (x = 0, 1) could be expected to subsequently oligomerize irreversibly and lead to the observed decomposition.

The Effect of Modifying Stoichiometries and Isolation Procedures in Reactions of $LnCl_3$ with $NaOCMe_3$. Although complexes **1** and **2** can be isolated in consistently high yields using the procedure described above, slight modifications of this procedure can greatly affect the outcome of the reaction. Complexes **1** and **2** are isolated by removing the reaction solvent (THF), washing with hexane, and extracting with toluene. A reasonable alternative isolation procedure is to first centrifuge the crude reaction mixture to remove insoluble byproducts, e.g., NaCl, and then remove the THF solvent, wash with hexane, and extract with toluene. However, when this superficially minor variation in isolation procedure is carried out, complexes **1** and **2** are not observed as reaction products. Instead, in both reactions, the ^1H NMR spectrum of the product showed only a single broad *tert*-butoxide resonance.

The importance of the isolation procedure became even more obvious when the reaction of $EuCl_3$ with 3 equiv of $NaOCMe_3$ was examined to see if trimetallic europium complexes analogous

to $La_3(OCMe_3)_9(THF)_2$[2] and $Y_3(OCMe_3)_8Cl(THF)_2$[3] could be obtained. As in the 10-equiv reaction, two different types of reaction products can be observed depending on which isolation procedure is followed. Following the procedure used to isolate **1** and **2**, the 3-equiv reaction formed $EuNa_8(OCMe_3)_{10}Cl$ (**1**) in up to 30% yield! The balanced equation necessary to obtain **1** from this 3-equiv reaction is given in reaction 6. This shows that a small amount of europium, under the proper conditions, can tie

$$EuCl_3 + 3NaOCMe_3 \rightarrow 0.3EuNa_8(OCMe_3)_{10}Cl + 0.7EuCl_3 + 0.6NaCl \quad (6)$$

up a large amount of alkoxide reagent, even in the presence of excess metal halide.

In contrast, when the alternative isolation procedure involving centrifugation followed by solvent removal, hexane wash, and toluene extraction was applied to the 3:1 $NaOCMe_3$:$EuCl_3$ reaction, complex **1** was not observed. Instead, a mixture of products was observed by ^1H NMR spectroscopy, which had spectral characteristics consistent with trimetallic complexes such as **4–6**. The ^1H NMR spectrum of the product mixture shows numerous resonances between 26 and −34 ppm.[22]

The above results suggest that equilibria are present in this $EuCl_3/NaOCMe_3$ system which can be shifted by isolation procedures to favor different products. The instability of **1** and **3** in THF-d_8 and the importance of thorough hexane washes in the procedure to make **1** and **2** suggest that **1–3** are formed in the isolation procedure as the THF is being removed.

Discussion

Synthesis. Several aspects of the synthetic chemistry presented above may have general implications in alkoxide chemistry and deserve discussion.

(a) The Existence of a New Class of Heterometallic Alkoxide Complexes. The reaction of $EuCl_3$ and YCl_3 with 10 equiv of $NaOCMe_3$ to form **1** and **2**, reaction 5, demonstrates a synthetic pathway to a new class of mixed-metal lanthanide alkali metal alkoxides. Prior to this work, reactions of YCl_3 with a stoichiometric excess of 4 equiv of $NaOCMe_3$ led primarily to insoluble products. It appeared that the range of soluble products accessible from the $YCl_3/NaOCMe_3$ system required 3 or less equiv of *tert*-butoxide. Obviously, by using a large excess of $NaOCMe_3$, one can move beyond this class of insoluble products to a new regime of alkoxide systems in which the complexes are again readily soluble. The high content of $NaOCMe_3$ in **1** and **2**, which can be formally written $(RO)_3Ln(NaOR)_7(NaCl)$, makes them quite similar to $(NaOCMe_3)_n$ as discussed below and suggests that it should be possible to incorporate a wider variety of metal alkoxides into poly-$NaOCMe_3$ frameworks. Hence, it may be possible to generate a variety of $(RO)_xM(NaOR)_y(NaZ)$ complexes using x-valent metals in which $y \gg x$ and Z is a monoanionic ligand such as Cl^- or OH^-.

(b) The Effect of Reaction Stoichiometry in *tert*-Butoxide Reactions. Obviously, the stoichiometry for a $LnCl_3/NaOR$ reaction can greatly affect the nature of the products. For YCl_3 and $NaOCMe_3$, three distinct stoichiometries have been shown to give three different products in high yield: 10:1 forms **2** (eq 5), 3:1 forms **4** (eq 1), and 2:1 forms **5** (eq 2). For the $EuCl_3/NaOCMe_3$ system, the situation is more complicated since **1** can be obtained from both 10:1 and 3:1 stoichiometries. What is less obvious, however, is that the existence of **1–3** raises the possibility that complexes of this type can form in other systems and tie up large amounts of alkoxide reagent. This could cause a drastic change in the effective alkoxide concentration and change the course of the reaction.

(c) The Effect of the Product Isolation Procedures. Adding to the uncertainty caused by the possibility of forming complexes like **1–3** is the variability in product distribution observed as a function of the isolation procedure. A similar situation has also been observed in the reaction of YCl_3 with NaC_5H_5 and the reaction of $(C_5H_5)_2YCl(THF)$ with NaOMe.[23] In both cases, removal of alkali metal salts by centrifugation before extraction gave different results from direct extraction of the crude reaction mixture. In those cases, these phenomena apparently occurred because of the existence of less soluble adducts of the expected products $(C_5H_5)_2YCl(THF)$ and $(C_5H_5)_2Y(OMe)(THF)$. These less soluble adducts apparently did not form as readily when stoichiometric amounts of NaCl were present. The reaction of $(C_5H_5)_2YCl(THF)$ with NaOMe was also shown to be highly sensitive to local concentrations of reagents. Changing the stoichiometry of the reaction by even 30% caused different reaction routes to be traversed.

The present study shows another example of the critical nature of the isolation procedure in getting a specific product. Clearly, removal of insoluble products by centrifugation interferes with the reaction pathways that lead to **1** and **2**. In the europium case, the instability of **1** in THF suggests that it may be formed during the isolation procedure when the amount of THF is reduced in the presence of all of the insoluble materials in the reaction. In general, this suggests that one of the important variables in developing a lanthanide alkoxide reaction system is the isolation procedure. A low yield may be increased by changing the method of product isolation or a new reaction product may be obtained.

Structural Features. The nonametallic structures found in **1–3** adopt one of the standard nine vertex geometries for polyelement assemblies, namely the capped square antiprism.[24] The lanthanide atom in the capping position at the top of the structures is formally six-coordinate if the central chloride or hydroxide is considered to be a ligand. Since six-coordination is commonly observed for yttrium in crystallographically-characterized *tert*-butoxide complexes[2-5,11] this is a reasonable assignment. Since the lanthanide metal in this type of complex is in a common coordination environment, it seems likely that this type of compound could readily form in other systems.

The nearly linear Ln–O(5)–C(5) angle for the terminal alkoxide in these complexes is oriented to maximize O–Ln π donation, but it is also oriented in the sterically most favored position. C(Me)···C(Me) nonbonding contacts of as close as 3.77, 3.67, and 3.84 Å in **1–3**, respectively, are found for the methyl groups attached to C(5) in these structures. Since the sum of a van der Waals radii for two methyl groups is 4 Å,[25] steric crowding may favor the nearly linear orientation.

The sodium atoms in **1–3** are four-coordinate if the central chloride or hydroxide is considered to be a ligand to each of the sodium sites. Since the overall Na–Cl average distance of 2.82(13) Å is equivalent to the 2.814-Å Na–Cl distance in NaCl,[20] this is not unreasonable. However, the Na–Cl distances fall into two distinct ranges with the upper four sodium atoms having 2.74(1)- and 2.65(1)-Å averages in **1** and **2** and the lower four sodium atoms having 2.90(2)- and 2.98(4)-Å averages. The top four sodium atoms should certainly be considered four-coordinate, but it may be more appropriate to consider the bottom four sodium atoms as three-coordinate. The average Na–O distances support

(22) The observed signals can be divided into two sets of five resonances (each displays a 2:1:2:1:1 pattern), one set of four resonances (2:2:2:1), and one set of six resonances (2:2:2:1:1:1). Since each set of resonances has been independently observed in other reaction mixtures, it is presumed that each set is associated with an independent complex. These patterns are consistent with a structure analogous to $Ln_3(OCMe_3)_{9-x}Cl_x(THF)_2$. ^1H NMR (THF-d_8): (a) 14.93 (s, 18H), −7.34 (s, 9H), −14.47 (s, 18H), −28.00 (s, 9H), −29.13 (s, 9H); (b) 11.21 (s, 18H), −15.45 (s, 9H), −20.20 (s, 18H), −20.28 (s, 9H), −26.07 (s, 9H); (c) 26.05 (s, 18H), 16.94 (s, 18H), −16.48 (s, 18H), −34.33 (s, 9H); (d) 18.49 (s, 18H), 1.16 (s, 18H), 0.86 (s, 18H), −13.89 (s, 9H), −21.08 (s, 9H), −32.75 (s, 9H).

(23) Evans, W. J.; Sollberger, M. S.; Shreeve, J. L.; Olofson, J. M.; Hain, J. H., Jr.; Ziller, J. W. *Inorg. Chem.* **1992**, *32*, 2492–2501.

(24) Favas, M. C.; Kepert, D. L. *Prog. Inorg. Chem.* **1981**, *28*, 309–367.

(25) Pauling, L. *The Nature of the Chemical Bond*, 3rd ed.; Cornell University Press: Ithaca, NY, 1960; p 260.

this assignment in that the Na–O(μ_3-$OCMe_3$) average distances for the top four sodium atoms are longer than those of the bottom four sodium atoms. However, the difference in these averages, 0.10 Å, is much larger than the 0.01–0.02 Å difference in radius which is found as the coordination number of sodium changes by one unit according to Shannon.[19]

The sodium part of the $LnNa_8(OCMe_3)_{10}Z$ complexes has similarities to the $(NaOCMe_3)_9$ part of the structure of $NaOCMe_3$.[21] The orientation of $(NaOCMe_3)_9$ in Figure 6 shows this similarity. One obvious difference between the $Na_9(anion)_9$ structure and the $LnNa_8(anion)_{11}$ structure is that the addition of the trivalent lanthanide requires two additional anionic ligands for charge balance. One of these can be considered to be the internal Z ligand and the other the terminal alkoxide on Y or Eu. The similarity in structures between $NaOCMe_3$ and **1–3** is probably due to the fact that these two "extra" ligands can be located internally and exopolyhedrally such that the basic structure is not greatly perturbed. In fact, if the *tert*-butoxide ligand at the bottom of Figure 6 were quadruply-bridging, as in **1–3**, the structures would be very similar. The origin of this difference must arise from the presence of the higher coordinate europium or yttrium heteroatom in **1–3**.

The nonametallic structure observed for **1–3** may prove to be quite general. Recently, a similar structure was reported for the mixed alkali metal enolate alkoxide complex $Li_4K_5(OCMe_3)_4(enolate)_4(THF)_5(OH)$[26] where the enolate anion is $OC(=CH_2)CMe_3^-$. This $M_9(anion)_9(neutral\ ligand)_5$ complex differs from the $M_9(anion)_{11}$ structures of **1–3** in that the four atoms at the bottom of the capped square antiprism have a terminal ligand each (THF) instead of one μ_4-alkoxide as in **3** and **4**. Otherwise, the structures are analogous. If there is a special propensity for this structural type to form, this provides an explanation for the incorporation of small ligands like chloride and hydroxide into **1–3**. A compound with the formula $LnNa_8(anion)_{11}$ could not have this structure if all of the anions were *tert*-butoxide ligands. The structure requires that one of the anions be small enough to be located internally.

(26) Willard, P. G.; MacEwan, G. J. *J. Am. Chem. Soc.* **1989**, *111*, 7671–7672.

Conclusion

This study has shown that a series of mixed-metal nonametallic complexes of general formula $LnNa_8(OCMe_3)_{10}X$ exists and can be readily formed under the appropriate conditions from $LnCl_3$ and $NaOCMe_3$. Given the similarity of these complexes to $(NaOCMe_3)_9$ and the structural flexibility exhibited, this class of mixed-metal complexes may be much more general than the examples described here. Clearly, the method of isolation of products from $LnCl_3/NaOCMe_3$ reactions must be carefully considered since it can greatly affect the outcome of a reaction. This study also demonstrates that ^1H NMR spectroscopy is useful in characterizing polymetallic europium alkoxide complexes.

Acknowledgment. We thank the Division of Chemical Sciences of the Office of Basic Energy Sciences of the Department of Energy for support (to W.J.E.) of this research.

Supplementary Material Available: Tables of complete crystallographic data, positional parameters, bond distances and angles, and thermal parameters (51 pages). Ordering information is given on any current masthead page.